

**Lipid chain-driven interaction of a lipidated Src-family
kinase Lyn with the bilayer membrane**

Journal:	<i>Organic & Biomolecular Chemistry</i>
Manuscript ID	OB-ART-06-2022-001079.R2
Article Type:	Paper
Date Submitted by the Author:	18-Jul-2022
Complete List of Authors:	Hanashima, Shinya; Osaka University, Department of Chemistry, Graduate School of science, Osaka University Mito, Kanako; Osaka Daigaku Umegawa, Yuichi; Osaka University, Department of Chemistry Murata, Michio; Osaka University, Graduate School of Science Hojo, Hironobu; Institute for Protein Research, Osaka University,

Lipid chain-driven interaction of a lipidated Src-family kinase Lyn with the bilayer membrane

Authors

Shinya Hanashima,^{1,*} Kanako Mito,¹ Yuichi Umegawa,¹ Michio Murata,^{1,2} Hironobu Hojo^{2,3}

Affiliations

1. Department of Chemistry, Graduate School of Science, Osaka University, 1-1 Machikaneyama-cho, Toyonaka, Osaka 560-0043, Japan
2. Forefront Research Center, Graduate School of Science, Osaka University, Toyonaka, Osaka 560-0043, Japan
3. Institute for Protein Research, Osaka University, Yamadaoka 3-2, Suita 565-0871, Japan

*Corresponding author

Shinya Hanashima

e-mail: hanashimas13@chem.sci.osaka-u.ac.jp

Abstract

N-myristoylation is a process of ubiquitous protein modification, which promotes the interaction of lipidated proteins on cell surfaces, in conjunction with reversible S-palmitoylation. We report cooperative lipid-lipid interaction of two acyl chains of proteins, which increases the protein–membrane interaction and facilitates selective targeting of membranes containing anionic lipids. Lyn is a member of the Src family kinases distributed on the membrane surface by N-myristoyl and neighbouring S-palmitoyl chain anchors at the unique N-terminus domain. We prepared N-terminal short segments of lipidated Lyn to investigate the behaviour of each acyl chain in lipid composition-dependent membrane interaction by solid-state nuclear magnetic resonance (NMR). Solid-state ^{31}P -NMR studies revealed that S-palmitoylation of N-myristoylated Lyn peptides increased the interaction between peptides and phospholipid head groups, particularly with the anionic phosphatidylserine-containing bilayers. The solid-state ^2H -NMR of Lyn peptides with a perdeutero N-myristoyl chain indicated an increase (0.6–0.8 Å) in the extent of N-myristoyl chain in the presence of nearby S-palmitoyl chains, probably through the interaction via the acyl chains. The cooperative hydrocarbon chain interaction of the two acyl chains of Lyn increased membrane binding by extending the hydrocarbon chains deeper into the membrane interior, thereby promoting peptide–membrane surface interaction between the cationic peptide side chains and the anionic lipid head groups. This lipid-driven mechanism by S-palmitoylation promotes the partition of the lipidated proteins to the cytoplasmic surface of the cell membranes, and may be involved in recruiting Lyn at the signalling domains rich in anionic lipids.

INTRODUCTION

Protein lipidation is a common posttranslational modification in eukaryotes, which regulates the functions and localization of proteins through membrane interactions and lateral diffusion.¹ The N-myristoyl chain in a protein is co-translationally installed at the exposed glycine residue upon removing the N-terminal methionine.² N-myristoylation is necessary but not sufficient for stable membrane binding because membrane association of myristoylated amino acids with a partition coefficient of about 10^{-4} is insufficient to evoke biological activities on the membrane.³ The unstable interaction of N-myristoylated proteins can be reinforced for their attachment to the membrane for a few days by S-palmitoylation of nearby cysteine residues and interaction between the positively charged amino acids cluster near the N-terminus with anionic membrane lipids.⁴ The reversible S-palmitoylation cycles, known as the myristoyl–palmitoyl switch,⁵ regulate the N-myristoylated proteins during membrane binding and trafficking,^{6, 7} interactions among lipidated proteins,⁸ and activity of proteins.⁹ In addition, lipid modification of protein therapeutics has the potential to facilitate targeting, prolong half-life, and decrease immunogenicity.¹⁰

Lyn is an N-myristoylated Src family tyrosine kinase (SFKs) recognized as a drug target¹¹ because of its role in leukaemia and solid cancers,¹¹ allergies,¹² and viral secretions.¹³ Lyn consists of a tyrosine kinase (SH1) domain at the C-terminus, followed by regulatory SH2 and SH3 domains and a unique SH4 domain.¹⁴ The domain sequences are highly conserved among SFKs except for the SH4 domain, and SH2 and SH3 domains regulate the kinase activity by interplaying with the active site of the SH1 domain.¹⁵ On the other hand, the unique sequences of the intrinsically disordered SH4 domain provide properties individual to the SFK members, including Lyn. The N-terminal glycine residue at the SH4 domain of Lyn undergoes N-myristoylation, and occasional S-palmitoylation at the neighbouring cysteine facilitates hydrophobic interaction within the hydrophobic interior of the inner leaflet membranes by increasing the acyl chain anchors. At the

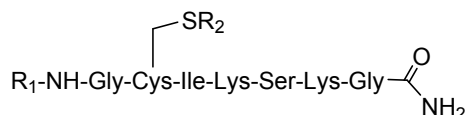
same time, the lysine and arginine stretch in the SH4 domain may promote membrane interaction through electrostatic binding with anionic lipid head groups, such as phosphatidylserines and phosphatidylinositides.^{16, 17} These lipidations can promote protein redistribution in the ordered domains such as lipid rafts,^{12, 18} and are probably involved in immune signalling through the very long acyl chain of lactosylceramide domain at the outer leaflet of immune cells.^{19, 20}

The acyl chain dynamics of lipidated peptides in model membranes has been investigated by solid-state ²H-NMR. The wobbling of peptide lipid chains was significantly affected by surrounding membrane lipid structures, such as the carbon number of the acyl chain, the degree of unsaturation, and the variety of head groups.²¹⁻²⁴ Previous ²H-NMR studies on palmitoyl Ras peptides in membrane bilayers indicated that the motion of the protein palmitoyl chain was similar to that of the surrounding dimyristoyl-glycero-phosphocholine.^{25, 26} However, for proteins with multiple lipidations, such as Lyn, the details of the acyl chain-dependent wobbling to increase the protein-membrane interaction have not been explored so far. Deuterated lipid probes with segment-specific labelling have been developed to examine lipid-lipid interactions,^{27, 28} dynamic lipid head group structure,²⁹ and membrane distributions by solid-state ²H-NMR.³⁰

Here, we examined membrane interaction of mono- and bis-acylated Lyn-heptapeptides (M-Lyn and MP-Lyn) (Fig.1) by focusing on the motions of methylene of each acyl chain using solid-state NMR. Seven amino acids at the N-terminus, including two lipidation sites and two lysine residues, were selected to acquire solid-state NMR data in two membrane conditions; the unitary POPC membranes and POPC/POPE/POPS (50:25:25) membranes. Because the intrinsically disordered SH4 domain connects the N-terminal lipidation segment to the structured domains of SFKs, we assumed that the short peptide segment could be a good model to examine the interaction of Lyn with the membranes. Solid-state ³¹P-NMR measuring *T*₁ relaxation time indicated that the bis-acyl Lyn peptide (MP-Lyn) significantly restricts the motion of phospholipid head groups compared with that done by the monoacyl Lyn peptide (M-Lyn), and prefers to bind the POPS/POPE component of the POPC/POPE/POPS membranes. Solid-state ²H-NMR coupling profiles of the Lyn

peptides having one perdeuterated myristoyl chain (M_d -Lyn and M_dP -Lyn) or perdeuterated palmitoyl chain (MP_d -Lyn) (Fig.1) were collected in the two-membrane systems and analysed by employing the mean torque model.³¹ The profiles indicated that S-palmitoylation of the N-acylated Lyn peptide extended the two acyl chains deeper into the membrane interior and thereby stabilized membrane binding of the bis-acyl peptide. The extended acyl chains of MP-Lyn in the membrane leaflet facilitate membrane interaction by increasing the hydrophobic matching within the membrane interior and promoting the interaction between cationic peptide moieties and the anionic lipid head groups on the membrane surface. The extended acyl chains of MP-Lyn within the inner leaflet may be prone to be involved in the leaflet coupling with a long fatty acid chain of the glycosphingolipid domain at the opposite leaflet relating to transmembrane signalling.

A



M_d -Lyn: $R_1 = d_{27}$ -myristoyl, $R_2 = H$

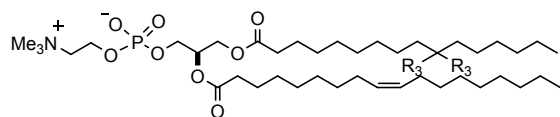
M_dP -Lyn: $R_1 = d_{27}$ -myristoyl, $R_2 =$ palmitoyl

MP_d -Lyn: $R_1 =$ myristoyl, $R_2 = d_{31}$ -palmitoyl

M-Lyn: $R_1 =$ myristoyl, $R_2 = H$

MP-Lyn: $R_1 =$ myristoyl, $R_2 =$ palmitoyl

B



POPC $R_3 = H$

$10',10''-d_2$ -POPC $R_3 = D$

Fig.1 The structures of the lipidated Lyn peptides (A) and $10',10''-d_2$ -POPC (B).

RESULTS

The interaction of Lyn peptides with lipid head groups examined by solid-state ^{31}P -NMR

We measured ^{31}P -chemical shift anisotropy (CSA) and spin-lattice (T_1) relaxation time of the phosphates on lipid heads to assess the changes in motion of lipid head groups by phospholipid-peptide interactions occurring on the membrane surface.³² The Lyn heptapeptides were synthesized in our laboratory and incorporated into the bilayer membranes.²² The CSA of the static ^{31}P -NMR for phospholipid membranes is sensitive to the order and orientation of the phosphate head groups and membrane curvature.

^{31}P -NMR spectral shapes indicated that the addition of 10 mol% lipidated Lyn peptides did not largely affect the dynamic lamellar structure in the POPC and POPC/POPE/POPS membranes at 30°C (Fig.2). The POPC/POPE/POPS membrane afforded three sets of ^{31}P -NMR CSA widths that were assignable to POPC (43.5 ppm), POPE (35.9 ppm), and POPS (54.5 ppm) (Fig.2D). The CSA values of all membrane conditions indicated that the lipidated Lyn-peptides did not greatly affect the head group orientation and order because the addition of Lyn-peptides altered the residual ^{31}P -CSA widths to less than a few ppm. On the other hand, the spectra of the POPC/POPE/POPS membranes were broadened in the presence of the M-Lyn peptide (Fig.2E) and further perturbed with the MP-Lyn peptide (Fig.2F), but were hardly affected in the POPC membranes (Fig.2B and C). These differences in signal broadenings suggest that the POPE/POPS component facilitates the interaction of the Lyn peptides with the membrane, and S-palmitoylation of M-Lyn increases the interaction of the peptide moiety with the lipid head groups on the membrane surface.

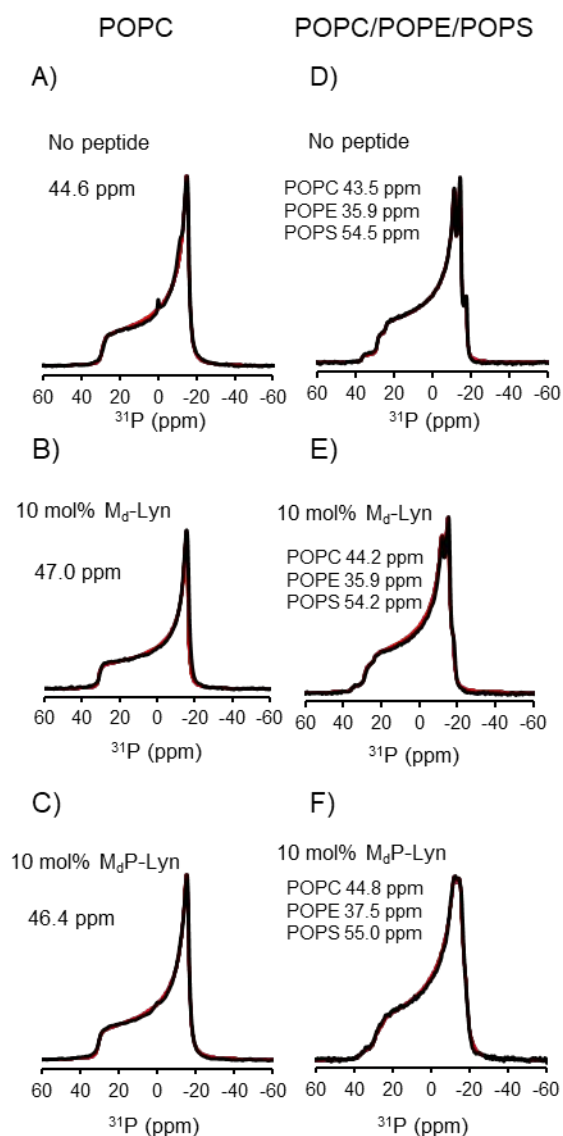


Fig.2 The effect of lipidated Lyn on solid-state ^{31}P -NMR spectra of the POPC (A–C) and POPC/POPE/POPS (D–F) membranes. A, D: phospholipid membranes without the peptides. B, E: membranes with 10 mol% $\text{M}_d\text{-Lyn}$. C, F: membranes with 10 mol% $\text{M}_d\text{P-Lyn}$. The black and red traces are the experimental and theoretical spectra. The spectra were collected at 30°C in static condition.

^{31}P -relaxation time is sensitive to the interaction of the phospholipid head groups with drugs and peptides that affect long axis rotation and membrane diffusion of lipids.³³ We observed the

dependence of ^{31}P T_1 relaxation time on the structures of the lipid head groups and acylation of peptides (Fig.3). Based on the temperature-dependent increase in the ^{31}P - T_1 relaxation time of the POPC/POPE/POPS membrane (Fig.S1), the decrease in T_1 implies a reduced phospholipid rotation and lateral diffusion caused by the interaction with the Lyn peptides.

In the POPC/POPE/POPS membrane, the ^{31}P -NMR signal of POPC was observed at -0.7 ppm, while POPE and POPS signals overlapped at -0.1 ppm under magic angle spinning (MAS) at 4 kHz (Fig.3A). As shown in Fig.3C, the T_1 relaxation times of both POPC and POPE/POPS signals in the POPC/POPE/POPS membrane decreased in the presence of M-Lyn. The decrease was more significant with MP-Lyn, indicating that S-palmitoylation to form MP-Lyn significantly perturbs the motion of the phospholipid head groups through peptide–membrane interaction. Furthermore, POPE/POPS signals from the POPC/POPE/POPS membrane showed a larger decrease in the T_1 relaxation time than that of the POPC signal, suggesting that the lipidated Lyn peptide prefers to interact with the POPE/POPS component. As shown in Fig.3B, the POPC membrane with the peptides showed small decreases in the T_1 relaxation times, consistently supporting the preference of Lyn-peptide for the POPE/POPS component. Therefore, S-palmitoylation of N-myristoylated Lyn enhances the interplay between peptides and lipid head groups on the membrane surface, particularly in the POPE/POPE/POPS membrane mimicking a typical lipid composition of the cytosolic leaflet of the plasma membrane.

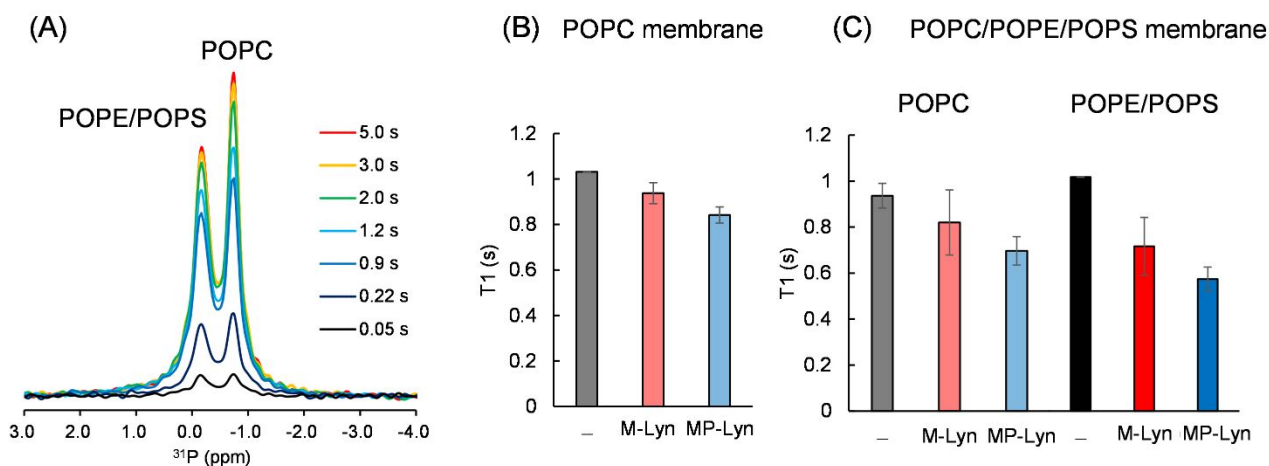


Fig.3 ^{31}P -NMR T_1 relaxation times of the POPC and POPC/POPE/POPS membranes with lipidated Lyn peptides at 30°C . A: Decay of the ^{31}P -MAS NMR spectra of the POPC/POPE/POPS membrane, including 10 mol% MP-Lyn. The spectra of each decay time were overlaid. T_1 relaxation times of POPE and POPS could not be distinguished owing to their ^{31}P -signal overlap. B,C: ^{31}P T_1 relaxation times of the POPC membrane and the POPC/POPE/POPS membrane with 10 mol% Lyn peptides. ^{31}P -NMR spectra were collected with 4 kHz MAS conditions at 30°C . — : no peptide. Each value represents the mean for 2–3 independent experiments with \pm standard deviation.

The extent of acyl chains of lipidated Lyn examined by ^2H NMR

The acyl chain dynamics in the membrane binding of the lipidated peptides was investigated using solid-state ^2H NMR. Solid-state ^2H NMR provides the quadrupolar coupling profiles originating from the wobbling degree of each CD_2 segment in perdeuterated acyl chains. According to the mean torque orientational distribution model,^{21, 31} these profiles can be translated into parameters to evaluate acyl chain stretching in the membranes. The solid-state ^2H NMR spectra of the three Lyn-peptides with perdeuterated acyl chains, $\text{M}_d\text{-Lyn}$, $\text{M}_d\text{P-Lyn}$, and $\text{MP}_d\text{-Lyn}$ (Fig.1), were collected in the unitary POPC and POPC/POPE/POPS membranes (Fig.4). The acyl chain parameters, area per chain (A_C), volumetric thickness (D_C), and acyl chain extent (L_C) (Fig.4H), were

deduced from the order parameter (S_{CD}).^{21, 31} S_{CD} was directly obtained from ^2H NMR quadrupolar coupling profile of the deuterated acyl chains (Fig.5).

All three lipidated Lyn peptides (10 mol% relative to the total lipid) were efficiently incorporated and dispersed in the POPC bilayers, therefore, showing a typical shape of the Pake doublets with an axially symmetrical pattern (Fig.4 A-C). The outermost peak of bis-lipidated $M_d\text{P-Lyn}$ showed larger quadrupolar coupling width (24.9 kHz) than the mono-lipidated $M_d\text{-Lyn}$ (20.8 kHz) (Fig.5A). This significant difference indicated that the S-palmitoyl chain decreased the mean segmental wobbling of the deuterated N-myristoyl chain of $M_d\text{P-Lyn}$. Namely, the S-palmitoylation extended the conformation of N-myristoyl chain of the peptide, resulting in a 2.7 \AA^2 smaller A_C and a 0.8 \AA longer L_C than those of $M_d\text{-Lyn}$ (Table 1). As shown in Fig.5B, the deuterated chains of $M_d\text{P-Lyn}$ and $MP_d\text{-Lyn}$ in the POPC membranes showed similar chain extent curves, and their outermost quadrupolar couplings were similar. The similarities between the N-myristoyl and S-palmitoyl chains of $MP\text{-Lyn}$ led to similar A_C 's (31.0 and 31.4 \AA^2). In contrast, the two extra methylene groups increased L_C of the S-palmitoyl chain (11.7 \AA) by 0.9 \AA compared to that of the N-myristoyl chain (10.8 \AA). The methyl terminus of S-palmitoyl chain of $MP\text{-Lyn}$ penetrated deeper into the bilayer interior when the carbonyl carbons of the palmitoyl and myristoyl chains were at close membrane depths.

^2H -NMR of the three deuterated Lyn peptides in the POPC/POPE/POPS membrane also showed the typical patterns of membrane-bound lipids (Fig.4D-F). A certain fraction of a broad shoulder in the $M_d\text{-Lyn}$ spectrum (Fig.4G) indicated that a part of $M_d\text{-Lyn}$ in this membrane probably formed rigid assemblages. The outermost width of $M_d\text{-Lyn}$ (24.3 kHz) dispersed in the POPC/POPE/POPS membrane (Fig.5C) was 3.5 kHz larger than that in the POPC membrane. This difference corresponds to a 0.9 \AA longer L_C (10.9 \AA) in the POPC/POPE/POPS membrane (Table 1). This increase implies the change of D_C , corresponding to the surrounding lipid membrane thickness (see next section). The extension of N-myristoyl chains by S-palmitoylation and the overlaid chain extent profile of the acyl chains of $MP\text{-Lyn}$ were observed in the POPC/POPE/POPS membrane

(Fig.5C,D). M_dP-Lyn in the POPC/POPE/POPS membrane showed a slightly extended myristoyl chain L_C at 11.4 Å, compared to that of M_d-Lyn (10.9 Å). The S-palmitoyl chain of M_dP-Lyn may interact with its own N-myristoyl chain, causing similar ordering effects on each other and resulting in nearly similar A_C values. The profiles of overlaid chain extents of M_dP-Lyn and MP_d-Lyn (Fig.5D) led to an S-palmitoyl chain 1.0 Å longer than the N-myristoyl chain (Table 1). Almost identical orders were noticed in the methylene segments with the same carbon number in each fatty acyl chain of MP-Lyn. Here, probably in the interaction between the N-myristoyl and S-palmitoyl chains assisted in embedding the segments with the same carbon number to a close membrane depth.

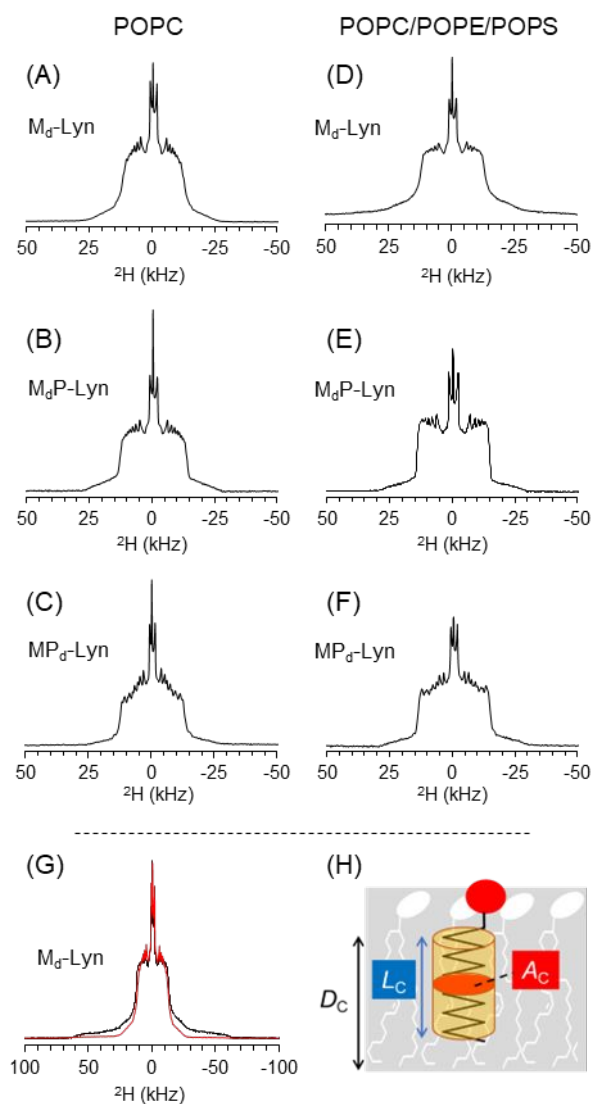


Fig. 4 ^2H NMR spectra of perdeuterated acyl chains of lipidated Lyn-peptides in the POPC (A, B, C) and POPC/POPE/POPS (50:25:25) membranes (D, E, F). The spectra of M_d -Lyn (A, D), M_dP -Lyn (B, E), and MP_d -Lyn (C, F) in the membranes were collected at 30°C. G: Overlay of the M_d -Lyn spectra in the POPC (red) and POPC/POPE/POPS (black) membranes with wider spectral ranges shown in A and D. H: The model showing area per deuterated chain (A_C), volumetric thickness (D_C), and the extent of peptide acyl chains (L_C).³¹

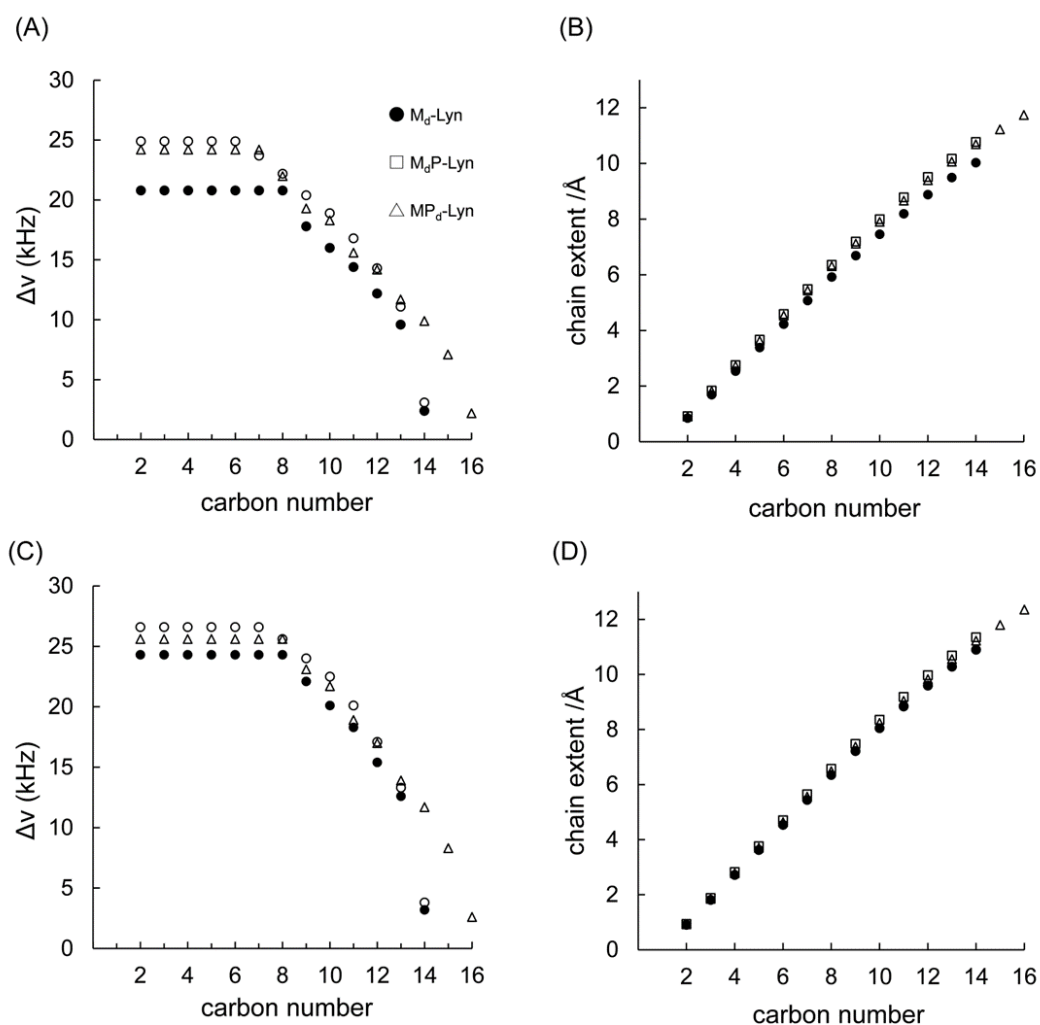


Fig.5 The quadrupolar coupling profiles (A, C) and extent (B, D) of the acyl chains of lipidated Lyn-peptides. A, B: The coupling profiles and chain extents of M_d-Lyn, M_dP-Lyn, and MP_d-Lyn in POPC membranes. C, D: The coupling profiles and chain extents in POPC/POPE/POPS membranes.

Effect of peptides on the acyl chains of surrounding membrane lipids

²H NMR spectra of 10',10'-d₂-POPC in each membrane system were collected to examine the effect of Lyn peptides on the surrounding phospholipids by observing the hydrocarbon chain wobbling at 10'-position (Fig.6). Position-selective deuteration of the acyl chains simplifies the ²H NMR

spectrum and minimizes the deuterium effect that influences lipid–lipid interaction.³⁴ Assuming that the 10' position is close to the maximum S_{CD} value,³⁵ the parameters of the hydrocarbon chains of POPC, such as A_C and D_C , were estimated from the S_{CD} values.³¹

The addition of M-Lyn to the POPC membranes did not affect the chain wobbling of surrounding POPCs because the quadrupolar coupling widths of 10',10'- d_2 -POPC (18.8 kHz) in the unitary POPC membrane containing 10 mol% M-Lyn (Fig.6A) was comparable to the widths without the peptide (Fig.S2). A slight increase in the coupling width of 10',10'- d_2 -POPC with 10 mol% MP-Lyn (Fig. 6B) indicated the negligible effect of MP-Lyn. As summarized in Table 1, the D_C value of 10',10'- d_2 -POPC in the POPC membrane was comparable to a reported value (13.5 Å) determined by X-ray scattering.³⁶ In the POPC/POPE/POPS membranes, 10',10'- d_2 -POPC with M-Lyn showed coupling widths 4.1 kHz larger than that in the unitary POPC membranes. This 1.2 Å increase in D_C value, corresponding to the value of the monolayer, was in agreement with a difference in the bilayer thickness (d_{HH}) of the POPC (37.5 Å) and POPC/POPE/POPS membranes (40.4 Å).³⁷ The bilayer thicknesses were assumed from the molar weighted average of membrane thicknesses estimated by previous molecular dynamic simulations; POPS (43.2 Å) and POPE (43.4 Å).³⁷ The partial assembly of M-Lyn forming an assemblage (Fig.4D) did not significantly affect the membrane bilayer structure, as obvious from the unchanged 2H -spectrum of 10',10'- d_2 -POPC (Fig.6C). The effect of MP-Lyn on the surrounding membrane lipids was also small in this membrane system (Fig.6D). Overall, the lipidated peptides in 10 mol% concentrations interacting with the lipid head groups did not significantly disrupt the hydrocarbon chain wobbling of surrounding lipid membranes. Small effects of the lipidated peptides on the ordering of surrounding phospholipids were also observed in previous reports using other membrane systems.^{22, 24}

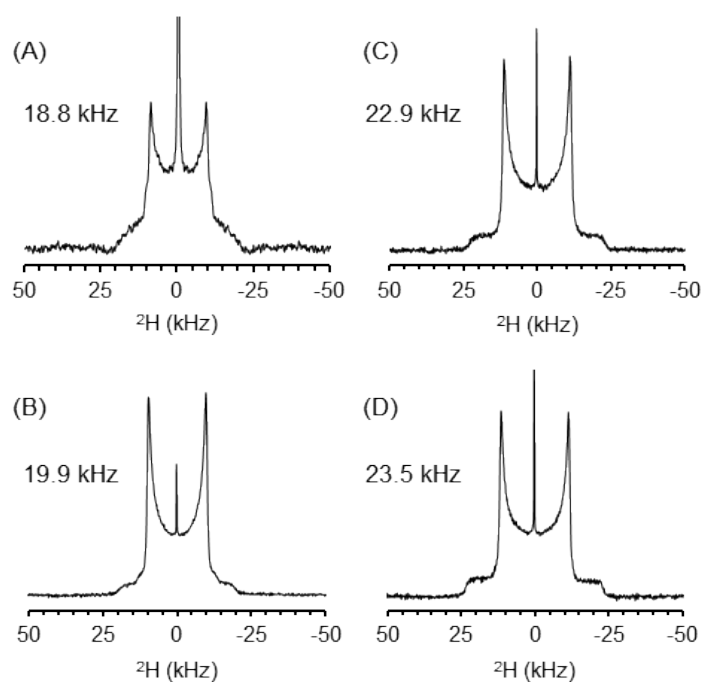


Fig.6 Solid-state ^2H NMR spectra of $10',10'\text{-}d_2\text{-POPC}$ in the unitary POPC membranes with M-Lyn (A) and MP-Lyn (B), and in the POPC/POPE/POPS membranes with M-Lyn (C) and MP-Lyn (D). POPC in the membranes was substituted with $10',10'\text{-}d_2\text{-POPC}$. All spectra were collected at 30°C .

Table 1. Summary of the lipid chain parameters (Fig.2G) derived from ^2H -NMR quadrupolar couplings.

membrane lipid	peptide (10 mol%)	deuterated probe	A_C (\AA^2)* ¹	D_C (\AA)* ²	L_C (\AA)* ³
POPC	—	$10',10'\text{-}d_2\text{-POPC}$	35.3	12.5	
	M-Lyn	$10',10'\text{-}d_2\text{-POPC}$	35.6	12.3	
		$M_d\text{-Lyn}$	33.7		10.0
	MP-Lyn	$10',10'\text{-}d_2\text{-POPC}$	34.5	12.7	
		$M_d\text{P-Lyn}$	31.0		10.8
		$MP_d\text{-Lyn}$	31.4		11.7
POPC/POPE/POPS	M-Lyn	$10',10'\text{-}d_2\text{-POPC}$	32.2	13.7	

50 : 25 : 25		M _d -Lyn	31.3	10.9
		10',10'-d ₂ -POPC	31.8	13.8
	MP-Lyn	M _d P-Lyn	30.1	11.4
		MP _d -Lyn	30.6	12.4

*¹: obtained from the largest S_{CD} of the perdeuterated chain of Lyn peptides or S_{CD} of 10',10'-d₂-POPC. *²: obtained from S_{CD} of 10',10'-d₂-POPC. *³: from S_{CD} values of methylene and terminal methyl groups.

DISCUSSION

The lipidated protein Lyn is a member of the SFKs that localizes in the inner leaflet of the plasma membrane, particularly at the lipid rafts,¹² and is involved in receptor-mediated signal transduction, known as myristoyl switches.³⁸ The lipid dynamics and binding depth of protein acyl chains are important for the affinity of lipidated proteins towards the membrane and their lateral diffusion. The binding depth also relates to the interleaflet lipid–lipid interactions and interdigitation,³⁹ which mediates the transfer of biological signals from one to the opposite leaflet.¹⁹ Furthermore, N-myristoylation is also involved in microbial and viral infections by assisting membrane association of pathogen proteins through lipidation.² N-myristoyltransferase and palmitoyl-acyltransferases are the potential targets in cancer therapy.^{40, 41} Therefore, protein lipidation is a potential target in chemotherapeutics.⁴² Understanding the mechanisms of protein lipidation-induced increase in affinity towards the membrane and distribution of lipidated proteins at the appropriate membrane domains are necessary.

S-palmitoylation of N-myristoylated proteins facilitates their membrane distribution through the myristoyl–palmitoyl switch.² The bis-acylation probably promotes membrane binding of the Lyn peptide because the palmitoyl chain, two carbons longer than the myristoyl chain, is better partitioned into the PC membrane with a stabilization energy of -6.9 kJ/mol.³ We deduce that the bis-acyl chains of the lipidated peptides increase the membrane affinity by increasing hydrophobic effect and by chain extension through interplaying each other. The chain interaction extended the

N-myristoyl chain of MP-Lyn by 0.8 Å in POPC membranes and by 0.5 Å in the inner leaflet mimicking POPC/POPE/POPS membranes compared to that of M-Lyn (Fig.7, Table 1). These increases theoretically corresponded to 0.5–1.0 segment per chain converted from *gauche* to *anti* conformation. The high thickness of the POPC/POPE/POPS membranes increased the extent of N-myristoyl and S-palmitoyl chains of MP-Lyn by about 0.6 and 0.7 Å, respectively. As shown in Fig.5B and 5D, the chain extent profiles of N-myristoyl and S-palmitoyl chains of MP-Lyn completely overlapped from C2 to C14 in both the POPC and POPC/POPE/POPS membranes owing to myristoyl chain stretching of MP-Lyn. This coincidence suggests that the N-myristoyl chain at the N-terminal glycine and S-palmitoyl chain at the side chain of Cys are positioned in the same manner along with the membrane depth (Fig.7).

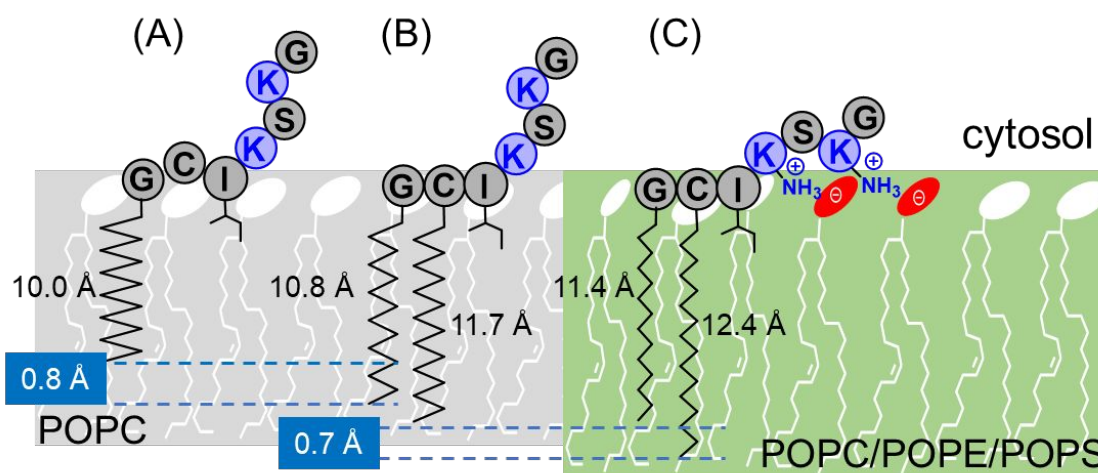


Fig. 7 Membrane association model of lipitated N-terminus of Lyn, depending on S-palmitoylation and membrane lipid components. A: M-Lyn in the POPC membrane. B: MP-Lyn in the POPC membrane. C: MP-Lyn in the POPC/POPE/POPS membrane. The hydrophobic side chain of Ile4 may also be involved in peptide-membrane interaction, like that observed for the Ras peptides.^{25, 26}

The N-myristoylated SFKs have several lysine and arginine residues within the N-terminal

20 residues (Lyn involves four lysine moieties). The electrostatic interaction of these cationic amino acids with the anionic lipid head groups assists the peptide–membrane binding as the myristoyl–electrostatic switch.² Here, the ³¹P-NMR line widths and *T*₁ relaxation times of the POPC/POPE/POPS membrane (Figs.2,3) indicate that the anionic head group of POPS interacts with the Lyn peptide likely using the lysines, and the electrostatic interactions play a certain role to increase the peptide-membrane interaction (Fig.7C). Furthermore, S-palmitoylation to form MP-Lyn significantly increased the binding with POPE/POPS component in the POPC/POPE/POPS membrane (Fig.3). Therefore, S-palmitoylation enhances lipidated protein–membrane interaction by increasing hydrophobic and electrostatic interactions. In addition, the SH4 domain of human Lyn has two potential phosphorylation sites, Ser11, and Ser13.^{43, 44} Phosphorylations of these serine residues nearby the cationic amino acids may reduce the binding with the anionic membranes known as the myristoyl–electrostatic switch of SFKs.⁴⁵

²H-NMR of M_d-Lyn indicates that M-Lyn forms aggregation in the POPC/POPE/POPS membrane but not in the unitary POPC membrane (Fig.4G, Fig.S4). The aggregation was mostly composed of M_d-Lyn without phospholipids, as evident from static ³¹P-NMR having no shoulder (Fig.2). Although N-myristoylation has been believed to improve membrane affinity, the underlying process may be complex. A similar result was reported for N-myristoylated guanylate cyclase-activating protein-2.²⁴ By contrast, the peptide bis-lipidation, increasing the hydrophobic effect, improved bilayer partition and distribution since M_dP-Lyn did not show aggregation in the POPC/POPE/POPS membrane (Fig.4E). These findings imply that the membrane lipid compositions and degree of lipid modifications are important factors in synergistical action of electrostatic interaction and hydrophobic effect. The potent homophilic interaction of M-Lyn to form aggregation in the membrane may also relate to forming membrane domains like the lipidated Ras proteins.^{46, 47} H-Ras is distributed at the interface of the liquid-ordered (Lo) and disordered (Ld) domains by the balance of two palmitoyl chains (Lo preferable) and one farnesyl chain (Ld preferable). The membrane cholesterol, known to be abundant at the lipid rafts, can increase the lipid chain ordering

in each leaflet by a fast flip-flop process,⁴⁸ and is thought to increase the order of the inner leaflet of raft domains.⁴⁹ The cooperative chain extension of the two Lo preferable acyl chains of Lyn and other SFKs possibly facilitate the distribution at the opposite leaflet of the lipid rafts. The inner leaflet of the lipid rafts, known to be enriched with anionic lipids,⁵⁰ likely prolongs the distribution of the SFKs through electrostatic interaction.

Lyn distributes at the cytosolic leaflet of the plasma membranes, which is highly enriched with unsaturated lipids,^{51, 52} and therefore highly fluidic and shows fast lipid diffusion.⁵³ In innate immunity, small lactosylceramide domains in the outer leaflet²⁰ are thought to transmit immune signaling via Lyn to the inner leaflet.⁵⁴ Lipidated Lyn at the inner leaflet may form nanoclusters as Ras proteins do.⁴⁶ The two saturated lipid chains may facilitate Lyn distribution to the opposite leaflet of the lactosylceramide domain for receiving transmembrane signal by the stretched acyl chains through inter-leaflet coupling.⁴⁹ Therefore, N-myristoylation and consequent S-palmitoylation of proteins, which trigger and regulate the membrane-binding through the myristoyl switch, are also assumed to be involved in localising the lipidated protein in the membrane domains enriched with anionic lipids, which can assist the transmembrane signalling.

Conclusion

Protein N-myristoylation at N-terminal glycine is a major co-translational modification that plays a fundamental role in membrane targeting and signaling through the so-called myristoyl switch, and is involved in cancers. Using solid-state NMR, our acyl chain-specific analysis of the heptapeptide segments of Lyn suggests a mechanistic insight into the S-palmitoylation-driven interaction of lipidated proteins with membrane lipids. The S-palmitoylation increases the order of the bis-acyl chain, and thereby facilitates the protein-membrane interplay and distribution of lipidated proteins into the functional membrane domains enriched in anionic lipids such as PS and phosphatidylinositol phosphates. The increased concentration of the lipidated proteins at a place for membrane functions may be involved in stable cell signalling through the membrane domains.

Author Contributions

S. Hanashima and M. Murata designed these experiments and wrote the manuscript. K. Mito synthesized lipidated peptides guided by H. Hojo. K. Mito and S. Hanashima performed NMR experiments and data analysis. Y. Umegawa assisted in NMR spectral analysis.

Conflicts of Interest

The authors declare no competing interests.

Acknowledgments

We are grateful for the discussions and suggestions by Profs. Nakayama and Iwabuchi, Juntendo University. We are also grateful for their technical assistance in solid-state NMR spectroscopy by Drs. Inazumi and Todokoro, Osaka University,. We also thank Ms. Mukogawa and Dr. Tsuchikawa in our laboratory to assist lipid synthesis. This work was supported in part by a Grant-in-Aid for Scientific Research JP19K05713 (S.H.), JP16H06315 (M.M.), and JP19K22257 (M.M.) from the Japan Society for Promotion of Science (JSPS), and CREST Grant Number JPMJCR18H2 (S.H.) from Japan Science and Technology Agency.

References

1. H. Jiang, X. Zhang, X. Chen, P. Aramsangtienchai, Z. Tong and H. Lin, *Chem Rev*, 2018, **118**, 919–988.
2. B. Wang, T. Dai, W. Sun, Y. Wei, J. Ren, L. Zhang, M. Zhang and F. Zhou, *Cell Mol Immunol*, 2021, **18**, 878–888.
3. R. M. Peitzsch and S. McLaughlin, *Biochemistry*, 1993, **32**, 10436–10443.
4. S. Shahinian and J. R. Silvius, *Biochemistry* 1995, **34**, 3813–3822.
5. M. D. Resh, *Prog Lipid Res*, 2016, **63**, 120–131.
6. O. Rocks, A. Peyker, M. Kahms, P. J. Verveer, C. Koerner, M. Lumbierres, J. Kuhlmann, H. Waldmann, A. Wittinghofer and P. I. H. Bastiaens, *Science*, 2005, **307**, 1746–1752.

7. K. Kasahara, Y. Nakayama, A. Kihara, D. Matsuda, K. Ikeda, T. Kuga, Y. Fukumoto, Y. Igarashi and N. Yamaguchi, *Exp Cell Res*, 2007, **313**, 2651–2666.
8. M. Matsubara, T. Nakatsu, H. Kato and H. Taniguchi, *Embo Journal*, 2004, **23**, 712–718.
9. O. Hantschel, B. Nagar, S. Guettler, J. Kretzschmar, K. Dorey, J. Kuriyan and G. Superti-Furga, *Cell*, 2003, **112**, 845–857.
10. R. Menacho-Melgar, J. S. Decker, J. N. Hennigan and M. D. Lynch, *J Control Release*, 2019, **295**, 1–12.
11. N. K. Williams, I. S. Lucet, S. P. Klinken, E. Ingley and J. Rossjohn, *J Biol Chem*, 2009, **284**, 284–291.
12. F. R. Maxfield and I. Tabas, *Nature*, 2005, **438**, 612–621.
13. M. Y. Li, T. S. Naik, L. Y. L. Siu, O. Acuto, E. Spooner, P. Wang, X. Yang, Y. Lin, R. Bruzzone, J. Ashour, M. J. Evans and S. Sanyal, *Nat Commun*, 2020, **11**, 5189.
14. S. M. Thomas and J. S. Brugge, *Annual Review of Cell and Developmental Biology*, 1997, **13**, 513–609.
15. T. J. Boggon and M. J. Eck, *Oncogene*, 2004, **23**, 7918–7927.
16. M. P. Pond, R. Eells, B. W. Treece, F. Heinrich, M. Losche and B. Roux, *J Mol Biol*, 2020, **432**, 2985–2997.
17. C. T. Sigal, W. Zhou, C. A. Buser, S. McLaughlin and M. D. Resh, *Proc Natl Acad Sci U S A*, 1994, **91**, 12253–12257.
18. J. H. Lorent and I. Levental, *Chem Phys Lipids*, 2015, **192**, 23–32.
19. H. Nakayama, M. Nagafuku, A. Suzuki, K. Iwabuchi and J. I. Inokuchi, *FEBS Lett*, 2018, **592**, 3921–3942.
20. S. Hanashima, R. Ikeda, Y. Matsubara, T. Yasuda, H. Tsuchikawa, J. P. Slotte and M. Murata, *Biophysical Journal*, 2022, **121**, 1143–1155.
21. A. Vogel, C. P. Katzka, H. Waldmann, K. Arnold, M. F. Brown and D. Huster, *J Am Chem Soc*, 2005, **127**, 12263–12272.
22. H. A. Scheidt and D. Huster, *Biophys J*, 2009, **96**, 3663–3672.
23. A. Gonzalez-Horta, D. Andreu, M. R. Morrow and J. Perez-Gil, *Biophys J*, 2008, **95**, 2308–2317.
24. A. Vogel, T. Schroder, C. Lange and D. Huster, *Biochim Biophys Acta*, 2007, **1768**, 3171–3181.
25. D. Huster, A. Vogel, C. Katzka, H. A. Scheidt, H. Binder, S. Dante, T. Gutberlet, O. Zschornig, H. Waldmann and K. Arnold, *J Am Chem Soc*, 2003, **125**, 4070–4079.
26. A. A. Gorfe, R. Pellarin and A. Caflisch, *J Am Chem Soc*, 2004, **126**, 15277–15286.
27. T. Yasuda, M. Kinoshita, M. Murata and N. Matsumori, *Biophysical Journal*, 2014, **106**, 631–638.
28. T. Yasuda, H. Tsuchikawa, M. Murata and N. Matsumori, *Biophysical Journal*, 2015, **108**, 2502–2506.

29. S. Hanashima, Y. Ibata, H. Watanabe, T. Yasuda, H. Tsuchikawa and M. Murata, *Org Biomol Chem*, 2019, **17**, 8601–8610.
30. S. Hanashima, K. Murakami, M. Yura, Y. Yano, Y. Umegawa, H. Tsuchikawa, N. Matsumori, S. Seo, W. Shinoda and M. Murata, *Biophysical Journal*, 2019, **117**, 307–318.
31. J. J. Kinnun, K. J. Mallikarjunaiah, H. I. Petrache and M. F. Brown, *Biochim Biophys Acta*, 2015, **1848**, 246–259.
32. A. Watts, *Bba-Rev Biomembranes*, 1998, **1376**, 297–318.
33. S. Abu-Baker, X. Qi and G. A. Lorigan, *Biophys J*, 2007, **93**, 3480–3490.
34. N. Matsumori, T. Yasuda, H. Okazaki, T. Suzuki, T. Yamaguchi, H. Tsuchikawa, M. Doi, T. Oishi and M. Murata, *Biochemistry*, 2012, **51**, 8363–8370.
35. A. Leftin, T. R. Molugu, C. Job, K. Beyer and M. F. Brown, *Biophys J*, 2014, **107**, 2274–2286.
36. N. Kucerka, S. Tristram-Nagle and J. F. Nagle, *J Membr Biol*, 2005, **208**, 193–202.
37. G. Shahane, W. Ding, M. Palaiokostas and M. Orsi, *J Mol Model*, 2019, **25**, 76.
38. E. Ingley, *Cell Commun Signal*, 2012, **10**, 21.
39. E. London, *Acc Chem Res*, 2019, **52**, 2382–2391.
40. E. Beauchamp, M. C. Yap, A. Iyer, M. A. Perinpanayagam, J. M. Gamma, K. M. Vincent, M. Lakshmanan, A. Raju, V. Tergaonkar, S. Y. Tan, S. T. Lim, W. F. Dong, L. M. Postovit, K. D. Read, D. W. Gray, P. G. Wyatt, J. R. Mackey and L. G. Berthiaume, *Nature Communications*, 2020, **11**, 5348.
41. M. S. Rana, P. Kumar, C. J. Lee, R. Verardi, K. R. Rajashankar and A. Banerjee, *Science*, 2018, **359**, eaao6326.
42. M. D. Resh, *Trends Mol Med*, 2012, **18**, 206–214.
43. F. S. Oppermann, F. Gnad, J. V. Olsen, R. Hornberger, Z. Greff, G. Keri, M. Mann and H. Daub, *Mol Cell Proteomics*, 2009, **8**, 1751–1764.
44. E. Kinoshita-Kikuta, T. Utsumi, A. Miyazaki, C. Tokumoto, K. Doi, H. Harada, E. Kinoshita and T. Koike, *Sci Rep*, 2020, **10**, 16273.
45. R. Roskoski, Jr., *Biochem Biophys Res Commun*, 2005, **331**, 1–14.
46. K. Weise, S. Kapoor, C. Denter, J. Nikolaus, N. Opitz, S. Koch, G. Triola, A. Herrmann, H. Waldmann and R. Winter, *J Am Chem Soc*, 2011, **133**, 880–887.
47. L. Janosi, Z. L. Li, J. F. Hancock and A. A. Gorfe, *P Natl Acad Sci USA*, 2012, **109**, 8097–8102.
48. W. F. D. Bennett, J. L. MacGillum, M. J. Hinner, S. J. Marrink and D. P. Tieleman, *J Am Chem Soc*, 2009, **131**, 12714–12720.
49. S. Chiantia and E. London, *Biophysical Journal*, 2012, **103**, 2311–2319.
50. L. J. Pike, *J Lipid Res*, 2003, **44**, 655–667.
51. J. H. Lorent, K. R. Levental, L. Ganesan, G. Rivera-Longworth, E. Sezgin, M. Doktorova, E. Lyman and I. Levental, *Nat Chem Biol*, 2020, **16**, 644–652.

52. M. Murate, M. Abe, K. Kasahara, K. Iwabuchi, M. Umeda and T. Kobayashi, *Journal of Cell Science*, 2015, **128**, 1627–1638.
53. A. Gupta, T. Korte, A. Herrmann and T. Wohland, *J Lipid Res*, 2020, **61**, 252–266.
54. E. Chiricozzi, M. G. Ciampa, G. Brasile, F. Compostella, A. Prinetti, H. Nakayama, R. C. Ekyalongo, K. Iwabuchi, S. Sonnino and L. Mauri, *J Lipid Res*, 2015, **56**, 129–141.